Anal. Bioanal. Electrochem., Vol. 16, No. 4, 2024, 360-376
https://www.doi.org/10.22034/abec.2024.712923

Analytical & Bioanalytical Electrochemistry

Full Paper

A Novel Voltammetric Sensor Based on $Tb_2(WO_4)_3$ Nanoparticles for Sulfadiazine Determination

Hana Beigizadeh, Mohammad Reza Ganjali*, and Parviz Norouzi*

Center of Excellence in Electrochemistry, School of Chemistry, College of Science, University of Tehran, Tehran, Iran

*Corresponding Author, Tel.: +98-61112294
E-Mail: ganjali@ut.ac.ir

Received: 16 November 2023 / Received in revised form: 10 April 2024 / Accepted: 14 April 2024 / Published online: 30 April 2024

Abstract- This work is focused on the development of a sensitive voltammetric electrode for sulfadiazine using nanoparticles of $Tb_2(WO_4)_3$ to modify a carbon paste electrode (CPE). The behavior of the modified CPE was evaluated through cyclic voltammetry (CV), electrochemical impedance spectroscopy (EIS), and fast Fourier transform square wave voltammetry (FFTSWV). The results revealed an irreversible sulfadiazine oxidation peak around 0.85 V *vs.* the Ag/AgCl reference electrode. The physicochemical properties of the nano-material were investigated using scanning electron microscopy (SEM), and X-ray powder diffraction (XRD). Some effective parameters such as, pH, percentage of modifier, amplitude, and frequency on sensor sensitivity were studied and optimized. The analytical curve was then obtained in the concentration ranges of 0.01–1.0 μM and 1.0–100 μM (with different sensitivity) with a detection limit of 4.10 nM by fast Fourier transform square wave voltammetry. Also, the electron transfer coefficient (α) was determined as a value of 0.66 for the sulfadiazine oxidation. The drug analysis in the pharmaceutical formulation was also carried out and recovery percentages in the range of 97–102% were recorded. The sensor presented good reproducibility and repeatability with acceptable RSD values (3.8%, 1.02% respectively) and long-term stability (almost one month).

Keywords- $Tb_2(WO_4)_3$ nanoparticles; Modified carbon paste electrode; Sulfadiazine; Fast Fourier transform square wave voltammetry

1. INTRODUCTION

Sulfonamides (Scheme 1) are sulfa drugs, that have received intense interest as an extensive gathering of engineered antibacterial compounds [1]. Despite the disclosure and wide utilization of different anti-microbials, these compounds are commonly used antibacterial agents prescribed for humans and animals [2], given their reasonable cost and effectiveness. Besides wide sulfonamides applications, they have the potential to show side effects such as susceptible and poisonous responses in patients. Therefore, having precise, simple, and sensitive techniques to track the drug residue would be a challenging task.

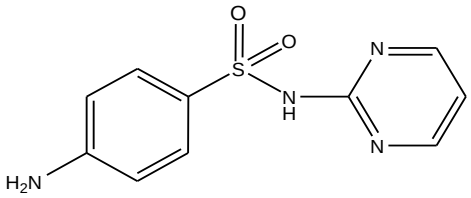

Scheme 1. Chemical structure of sulfadiazine

Sulfonamide is an electroactive compound since the $–NH_2$ and $–SO_2NH–$ groups can be oxidized and reduced, respectively [3]. Sulfadiazine is classified as one of the few sulfa-drugs that have been used broadly. Among applied methods used for sulfadiazine determination, spectrophotometry [4], various chromatography techniques e.g. HPLC, LC/MS, GC [5-10], and capillary electrophoresis with different detectors [3,11] can be mentioned. Also, electrochemical routes have been used for determining sulfonamides [12-20]. Electroanalytical techniques would not face many drawbacks of conventional techniques as they have accuracy, precision, sensitivity, and selectivity as advantages.

SWV is a powerful electrochemical technique widely used for analyzing of several compounds [12]. The detection limits in SWV measurements can be drastically improved by applying the Fast Fourier transform (FFT) to the SWV technique. In this approach, using the discrete FFT method signal and noise separation was performed in the frequency domain. Hence, the filtrations in some of the environmental noises from voltammetric signals cause an improvement in the limit of detection [13]. Using FFT technique coupled with an appropriate electrochemical method was found very sensitive system for trace analysis of several compounds based on the records [14-25].

Somehow, the lack of high sensitivity in trace analysis was compensable by electrode modification. Among various types of working electrodes, carbon paste electrodes (CPE) have been the subject of different research given their advantages of easy fabrication, wide potential range, fast surface renewal, and non-costly. However, modification of the working electrode was an excellent solution to overcome the high overpotential and low electron transfer kinetic problems of analyte electrochemical reactions [26-28]. The modifier properties can strongly

affect the response of modified carbon paste toward analytes. Recently various nanostructured materials have been utilized as modifiers due to their electrocatalytic activity and enhancing effects on the surface area of the unmodified electrode materials that increase the sensitivity of the electrochemical method [29,30].

Lanthanide elements series possess specific photogenic, magnetic, mechanical, and nuclear properties which have made them suitable for a wide range of uses in various areas like glass and ceramic manufacturing, metallurgy, and electronics [31]. Five electroactive elements of lanthanids (Ce, Sm, Eu, Tb, and Yb) could potentially be employed in voltammetric sensors. Among these elements terbium is also applicable in industry such as sonar systems, detectors, and sensors, as well as in fluorescent and colour TV lamps and tubes [32].

In the present study, the $Tb_2(WO_4)_3$ nanostructure-modified CPE was fabricated as the pharmaceutical sensor for sulfadiazine. The modified electrode was also used for trace analysis of sulfadiazine in pharmaceutical formulation. The application of the introduced modified electrode in real sample analysis was carried out using FFTSWV. Combining FFT techniques with electrochemical methods can lead to a highly sensitive technique in which noise is reduced significantly and the signal/noise (S/N) is enhanced [25,33].

2. EXPERIMENTAL SECTION

2.1. Chemicals

Sulfadiazine ((4-amino-N-2-pyrimidinyl) benzene sulfonamide) tablets were the products of a Local company, Tehran, Iran. All chemicals and solvents, high purity paraffin oil, graphite powder, potassium hexacianoferrate(II) trihydrate and hexacianoferrate(III) (i.e $(K_4[Fe(CN)_6].3H_2O)$, $(K_3[Fe(CN)_6])$, $Tb(NO_3)_3.6H_2O$ and $Na_2WO_4.2H_2O$) were obtained from Merck Co. A 1.0×10^{-3} M sulfadiazine solution was freshly prepared in a phosphate buffer solution (PBS) and used to prepare the rest of the solutions. The 0.01 M PBS was prepared by using standard NaH_2PO_4 and Na_2HPO_4 solutions. The pH of the solutions was adjusted to the required value using a sodium hydroxide solution.

2.2. Instruments

The PalmSens potentiostat (Palm Instruments BV) was used for EIS analyses. CV and FFTSWV were performed by a homemade electrochemical system made at the Centre of Excellence in Electrochemistry (CEE) at the University of Tehran. An A/D board was used to acquire the current data. Figure 1, illustrates the potential waveform which was applied to the working electrode. The software used for collecting and analysis of the electrochemical data was developed in Delphi 6.0. Using a bare (3-mm i.d.) or modified carbon paste working electrode, a graphite wire (auxiliary electrode) and reference (saturated Ag/AgCl) electrode were used to set up a three-electrode system used for the analyses.

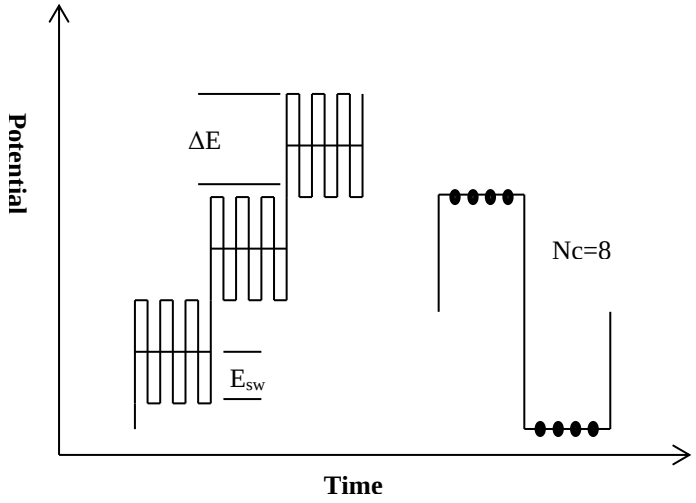

Figure 1. Potential wave response *vs.* time in SWV

2.3. Synthesis of the nanoparticles

A hydrothermal reaction between the cation and anion solutions was used to prepare the nanoparticles [34]. To this end 0.1 M tungstate and terbium solutions were prepared. 0.2 g of SDS, Triton X-100, and PVA (templating reagents) were dissolved in the tungstate solutions. The cation solution was added to that of the anion and the mixture was constantly stirred to obtain a suspension, which was next subjected to thermal treatment for 15 hours at 170 °C using an electric oven. Then the product was separated through centrifuging. The powder was next cleaned with ethanol and distilled water several times. At the end, the product dried at 80 °C for 4h. Table 1 shows the obtained results in different reaction conditions.

Table 1. Synthesis conditions applied to the synthesis of $Tb_2(WO_4)_3$ nanostructures

Sample no.	**Terbium (III) concentration (M)**	**Tb^{3+}: WO_4^{2-} molar ratio**	**Template**	**Morphology**
1	0.1	2:3	-	Particle
2	0.1	2:3	SDS	Coral-like
3	0.1	2:3	PVA	Sea urchin-like
4	0.1	2:3	Triton X-100	Wheat cluster-like

2.4. Modification of the electrodes

In each experiment, 0.1 g of the carbon paste was prepared using paraffin oil and graphite powder at 70/30 (w/w). This paste was then packed into a plastic tube (3-mm i.d.) and an

external contact was established by inserting a copper wire into the opposite end of the electrode through the opposite side of the tube. The surface of the resulting electrode was next carefully polished using a clean piece of paper. The modified CPEs were prepared as mentioned above in addition of adding 3, 5, or 7% of the $Tb_2(WO_4)_3$ to the paste. The selected 5% $Tb_2(WO_4)_3$ modified CPE was prepared by mixing 66.5/28.5/5 (%w/w/w) graphite powder/paraffin oil/ $Tb_2(WO_4)_3$. The new surface of the working electrode was gained by polishing after each signal recording.

2.5. Real sample preparation

Sulfadiazine tablets containing 500 mg of the medication were purchased. Ten tablets were carefully powdered and used to prepare solutions in PBS (pH=10.0) under sonication for 5 minutes. The prepared solution was used as the stock solution in the diluted analysis steps. The standard addition technique was used employed determine the recovery values through triplicate analyses.

3. RESULTS AND DISCUSSION

3.1. Characterizing the $Tb_2(WO_4)_3$ nanoparticles

To characterize, $Tb_2(WO_4)_3$ nanoparticles prepared without using templating agents (sample a) were utilized. Figure 2 represents the XRD pattern of $Tb_2(WO_4)_3$ nanoparticles. The sharp XRD peaks observed for the optimal nanoparticles were in complete agreement with the standards patterns reported for the $Tb_2(WO_4)_3$ sample in PC-APD; diffraction software (No. 00-028-1290).

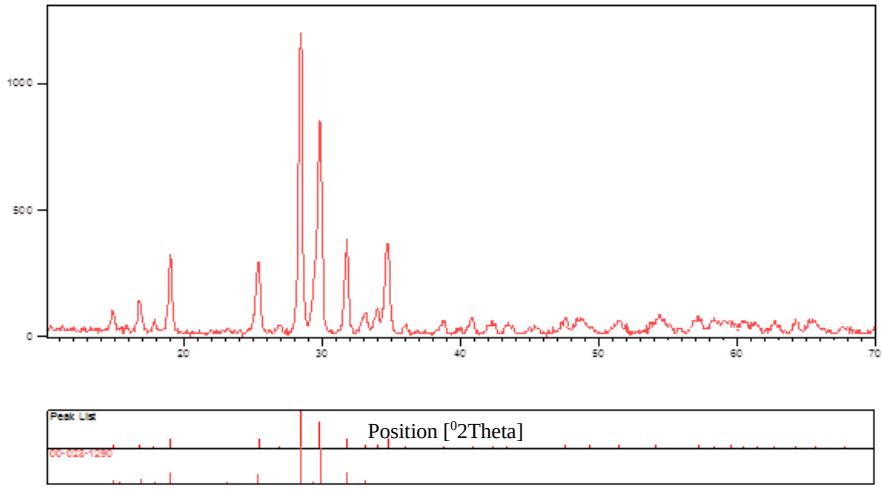

Figure. 2 XRD pattern for synthesized $Tb_2(WO_4)_3$ nanoparticle

Figures 3(A–D) show the SEM images of the nanostructures prepared by using different templating agents. According to Figure 3, different surfactants cause preparation of various morphology of resulted products and using no templating agent resulted in particle morphology of terbium tungstate with size around 50–60 nm. Applying SDS, PVA, and Triton-X100 as surfactants resulted in coral-like, sea urchin-like, and wheat cluster-like $Tb_2(WO_4)_3$, respectively. These indicate that the different agents led to different morphological properties in the products.

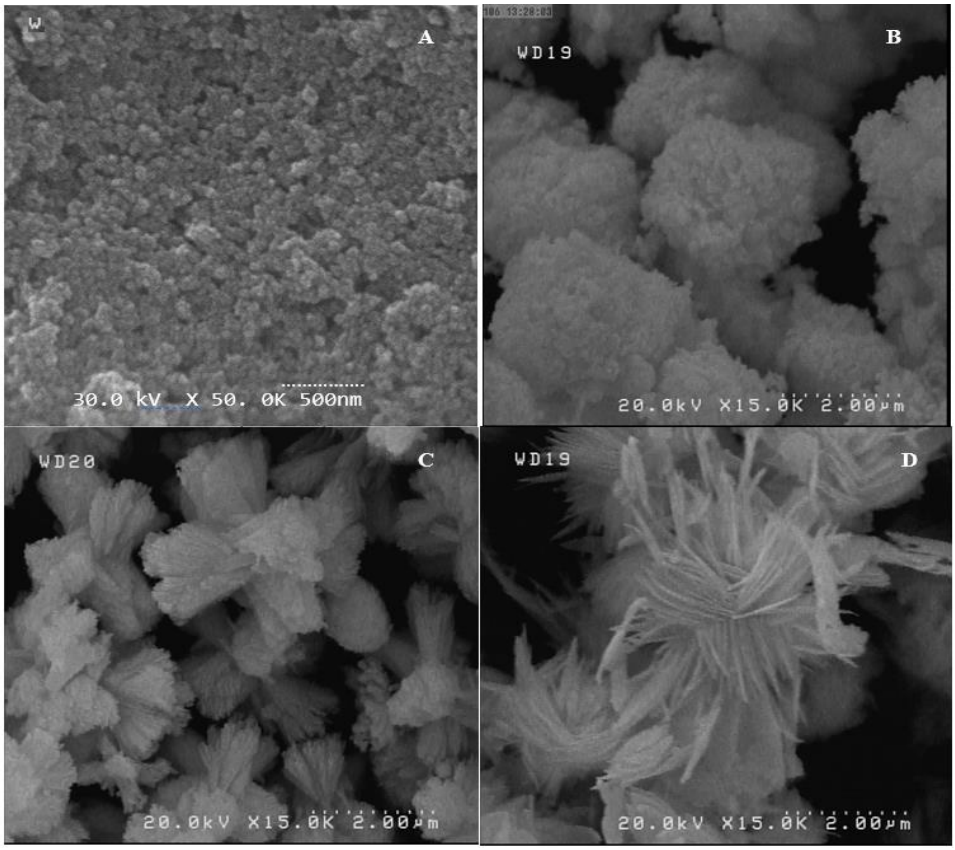

Figure 3. The scanning electron microscopy images of the $Tb_2(WO_4)_3$ nanostructures prepared through the hydrothermal method; A) in the absence of templates; B) using SDS; C) Triton x-100; D) PVA

3.2. Electrochemical impedance spectroscopy analysis

For the purpose of studying the impact of $Tb_2(WO_4)_3$ nanomaterials on the interfacial characteristic of the surface-modified carbon paste electrodes, cyclic voltammetry, and electrochemical impedance spectroscopy were employed [35]. In this experiment the bare CPE and CPE modified with $Tb_2(WO_4)_3$ nanostructures with different morphologies were utilized as working electrodes in a 1×10^{-3} M solution of $[Fe(CN)_6]^{3-/4-}$ also containing 0.1 M of KCl.

The cyclic voltammograms in Figure 4A show that the peak currents were enhanced at all modified electrodes. Besides, the lower peak-to-peak potential separation (ΔE_p) was achieved

using $Tb_2(WO_4)_3$ nanoparticles concerning the bare CPE. Using $Tb_2(WO_4)_3$ nanoparticle with all morphologies resulted in higher peak currents and the lower ΔE_p for $[Fe(CN)_6]^{3-/4-}$ redox probe. The results indicate that nanoparticle morphology could effectively accelerate the charge transfer to intensify the electrochemical signal due to its high conductivity and large specific surface area.

The electroactive surface area was calculated for the bare and modified CPE by applying the Randles-Sevcik equation [36]: $I_p = (2.69 \times 10^5)\ n^{3/2}\ A\ D^{1/2}\ C\ \nu^{1/2}$, where Ip refers to the peak current; n is the electron transfer number; A is the electroactive surface area (cm^2); D is the diffusion coefficient ($7.6\times10^{-6} cm^2 s^{-1}$ for 5 mM $[Fe(CN)_6]^{3-}$ ion in KCl 0.1 M); C is the concentration of $K_3[Fe(CN)_6]$ (M) and ν is the potential scan rate ($V\ s^{-1}$). The average estimated values (n = 3) for the active surface area were 0.045, 0.061, 0.066, 0.076, and 0.091 cm^2 for the bare CPE, $Tb_2(WO_4)_3$ nanowheat cluster, nanosea urchine, nanocoral and nanoparticle modified CPE, respectively. The results indicated the $Tb_2(WO_4)_3$ nanoparticle could improve the electrode surface's effective area.

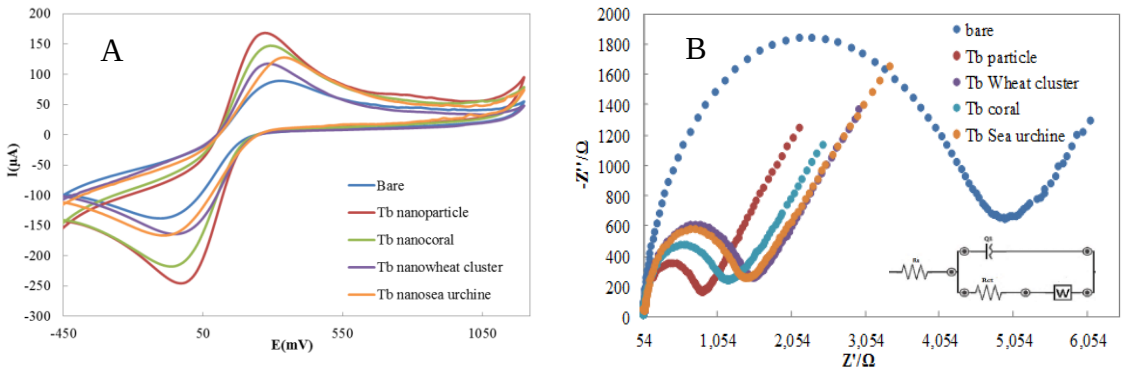

Figure 4. (A) Cyclic voltammograms (at 100 mVs^{-1}) and (B) Nyquist plots of the bare CPE and $Tb_2(WO_4)_3$ nanostructures modified CPE in the presence of 1×10^{-3} M $[Fe(CN)_6]^{3-/4-}$ in a 0.1 M KCl solution; Inset: equivalent circuit for the system

The Nyquist plots of acquired data are illustrated in Figure 4B. The best equivalent circuit with respect to the impedance data properly was represented in the inset of Figure 4B. The fitted equivalent circuit contains R_s, Q, R_{ct} and W which are symbols for the solution resistance, double-layer capacitance, charge transfer resistance and Warburg impedance. The Nyquist plot consist of two part, the semicircular and linear sections occurring at higher and lower frequencies correspond to the limiting charge transfer processes (the interfacial Rct of the redox reaction), and the mass diffusion limited process, respectively. The obtained values for the charge transfer resistance (R_{ct}) at modified electrodes vary with changes in $Tb_2(WO_4)_3$ morphologies. The gained quantity for the semicircles portion (R_{ct}) in the Nyquist plots, were 4940, 1500, 1400, 1141, and 816 Ω for the bare CPE, $Tb_2(WO_4)_3$ nanowheat cluster,

nanosea urchine, nanocoral and nanoparticle modified CPE, respectively. The drastic decrease in R_{ct} for $Tb_2(WO_4)_3$ nanoparticles modified CPE implied the electrocatalytic ability and higher conductivity of this electrode.

3.3. Electrochemical studies

The behavior of sulfadiazine on the surface of the $Tb_2(WO_4)_3$ nanostructures modified electrodes with all of the different morphologies was evaluated. Regardless to the morphology, all forms of the $Tb_2(WO_4)_3$ nanostructures presented the catalytic current response for the oxidation of sulfadiazine (Figure 5). Among the morphologies, $Tb_2(WO_4)_3$ nanoparticles showed the highest catalytic current (180 μA) for the oxidation of 1.0 mM sulfadiazine. The $Tb_2(WO_4)_3$ nanocoral-like, nanourchin-like and nanowheat cluster-like showed lesser catalytic currents of 120, 90, and 80 μA, respectively. The higher catalytic performance of the nanoparticles may be attributed to the high surface/volume and smaller-sized nanostructures compared to the other morphologies.

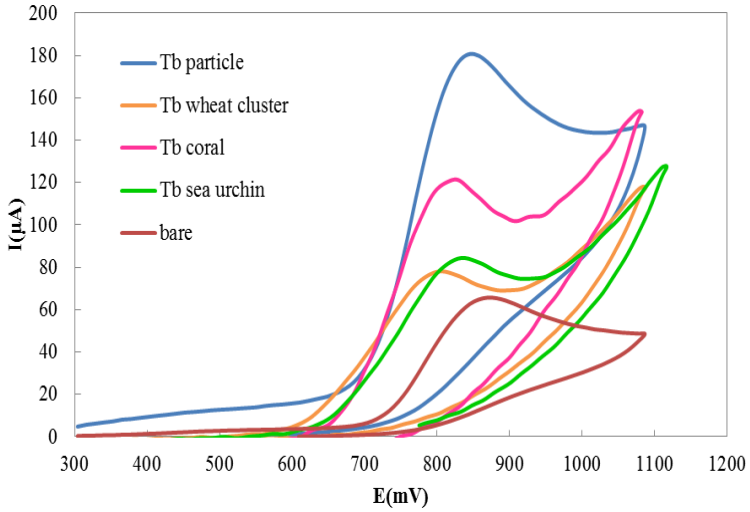

Figure 5. Cyclic voltammograms recorded at bare CPE and CPE electrodes modified using $Tb_2(WO_4)_3$ nanoparticle (blue line), nano coral like (pink line), wheat cluster like (orange line) and sea urchin like (green line) in the presence of 1.0 mM of sulfadiazine in PBS (pH=10.0) at 100 mVs^{-1}

3.4. The influence of modification

The effect of incorporating $Tb_2(WO_4)_3$ nanoparticles in the electrodes was also evaluated. To this end, four electrodes with different percentages of $Tb_2(WO_4)_3$ was constructed. The results obtained for different electrodes are illustrated in Figure 6.

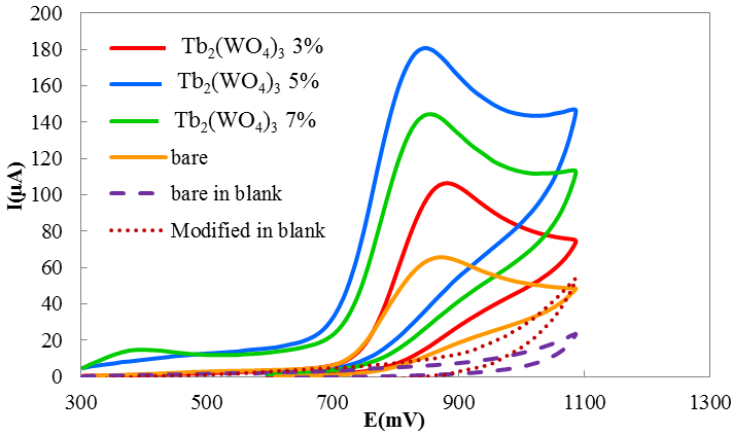

Figure 6. CVs were obtained using different electrodes. Unmodified CPE (orange line), 3% $Tb_2(WO_4)_3$/CPE (red line), 5% $Tb_2(WO_4)_3$/CPE (blue line), 7% $Tb_2(WO_4)_3$/CPE (green line) electrodes in 1.0 mM sulfadiazine, bare (dash line) and modified (dotted line) in absence of sulfadiazine in 0.01 M PBS solutions (pH 10.0), scan rate: 100 mVs^{-1}

No peak was identified in the absence of sulfadiazine, on both bare and modified electrodes. As can be seen, by increasing $Tb_2(WO_4)_3$ in the CPE composition, the current response was enhanced and the highest value was recorded for the electrode containing 5% (w/w) of $Tb_2(WO_4)_3$. Yet, further increasing this value weakens the oxidation peak current, which could be due to the lower conductivity and the electron transfer properties of the electrode surface. Consequently, the 5% (w/w) was chosen as a suitable amount of the $Tb_2(WO_4)_3$.

3.5. Effect of pH

The influence of pH on the response of the modified electrode in the pH window between 8 to 11 was investigated in a solution of 1.0 mM sulfadiazine and 0.01 M PBS (Figure 7). Based on Scheme 2, alkaline rezones were needed to solve sulfadiazine active ingredient.

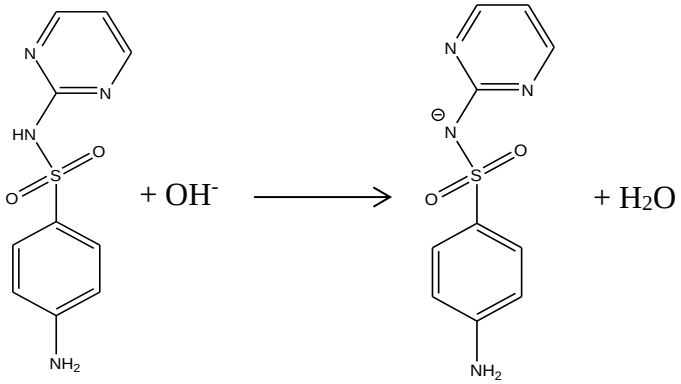

Scheme 2. Proposed reaction for solvation of sulfadiazine in alkaline media

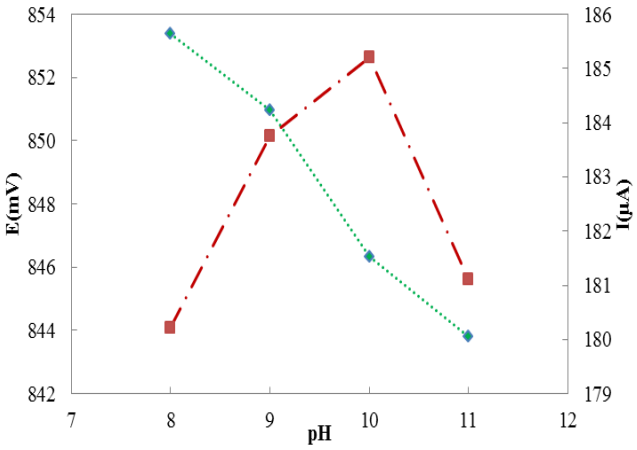

Figure 7. Plot of pH vs. peak current (red line dotted line) and potential (green dotted line) for $Tb_2(WO_4)_3$/CPE at various pH values, at 100 mVs^{-1}

E_p of sulfadiazine shifted to more negative values while the pH increased and the current density increased from pH 8.0 to 10.0 and then decreased. According to Scheme 3, the negative observed shift in the potential indicates the participation of protons in the electrode reaction process and that the oxidation of sulfadiazine is thermodynamically favored with the increase in pH.

The maximum peak currents response for sulfadiazine was recorded at pH 10.0. For this reason, pH 10.0 was selected as the best pH for further studies.

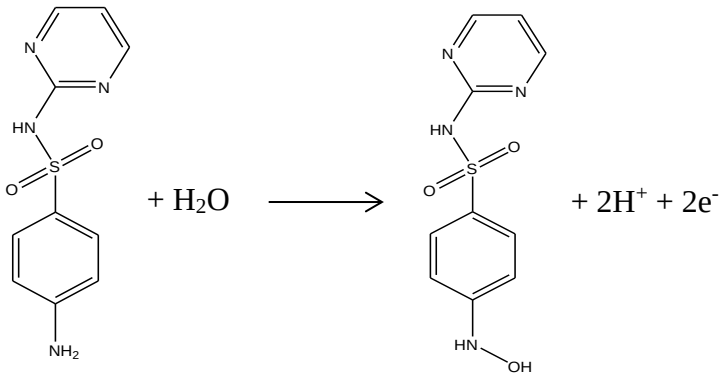

Scheme 3. Proposed reaction for electro-oxidation of sulfadiazine

3.6. Influence of the scan rate

The potential scan rate vs. oxidation current profile was recorded between 10 to 1000 mV s^{-1} using a 1.0 mM sulfadiazine solution in 0.01 M PBS (pH=10.0) and the results are presented in Figure 8. The peak maximum current vs. the square root of the scan rate forms a line (Figure 8B) reflecting the fact that the oxidation of sulfadiazine is diffusion controlled. Using the slope

of the plot of anodic peak potentials vs. logarithm of sweep rate (Figure 8C) based on Laviron equation [37], the charge transfer coefficient (α) was determined. In the case of anodic peaks, the slope of the linear section is 2.303RT/ (1– α) nF. Oxidation of sulfadiazine was two-electron process based on previous report [38] therefor the anodic transfer coefficient (α_a) was 0.66.

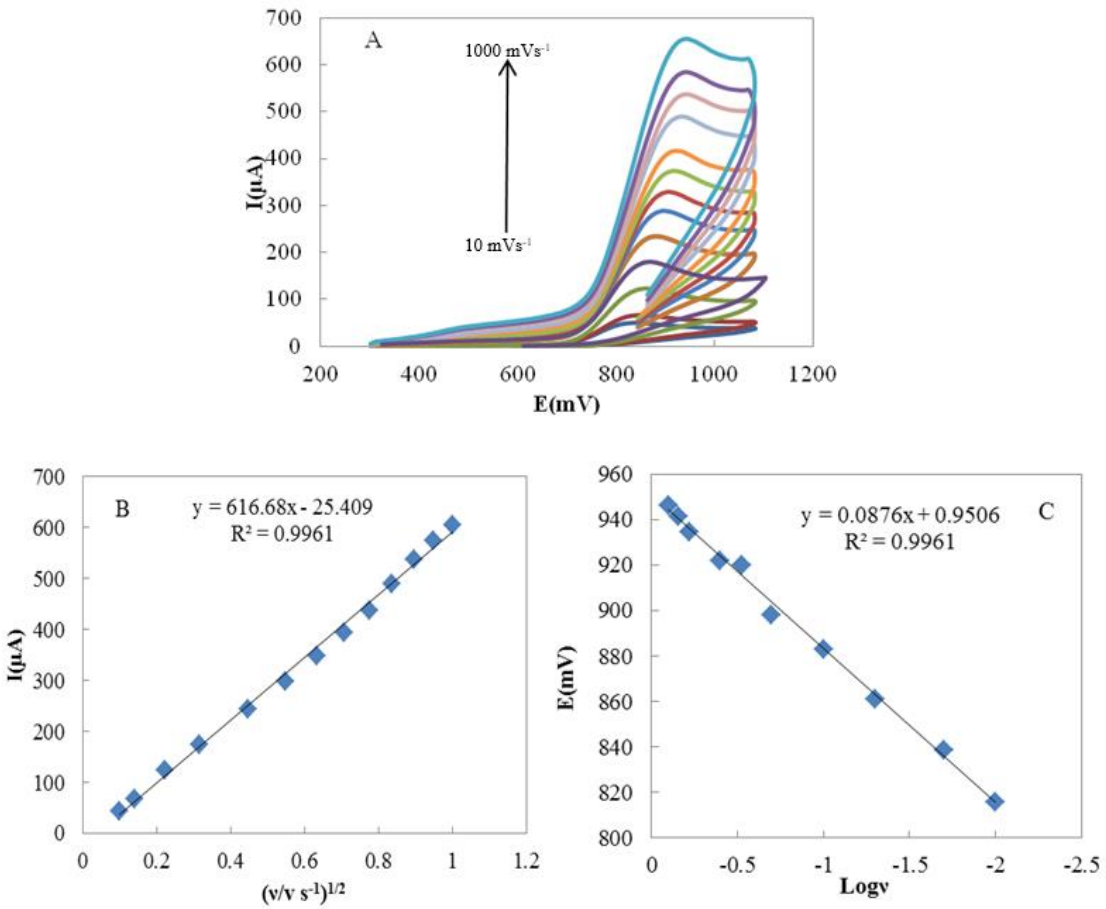

Figure 8. (A) CVs obtained using the $Tb_2(WO_4)_3$/CPE in a 0.1mM solution of sulfadiazine in a 0.01M PBS (pH=10.0) at various sweep rates, from inner the plot correspond to 10, 25, 50, 100, 200, 300, 400, 500, 600, 700, 800, 900 and 1000 mVs^{-1} scan rates, respectively; (B) Variations of peak current versus square root of sweep rates (C) Variation of E_p versus the logarithm of the sweep rate

3.7. Optimization of the FFTSWV parameters

The applicability of the modified CPE in the FFTSWV of sulfadiazine was evaluated. It is known that the FFTSWV response is affected by operating parameters such as frequency (f) and amplitude (E_{sw}). To study the effects of these factors on the response tests were run using a 0.1 mM solution of sulfadiazine in 0.01 M PBS (pH=10.0) and the results (Figure 9) indicated the optimized values for the frequency and amplitude to be 354 and 15, respectively.

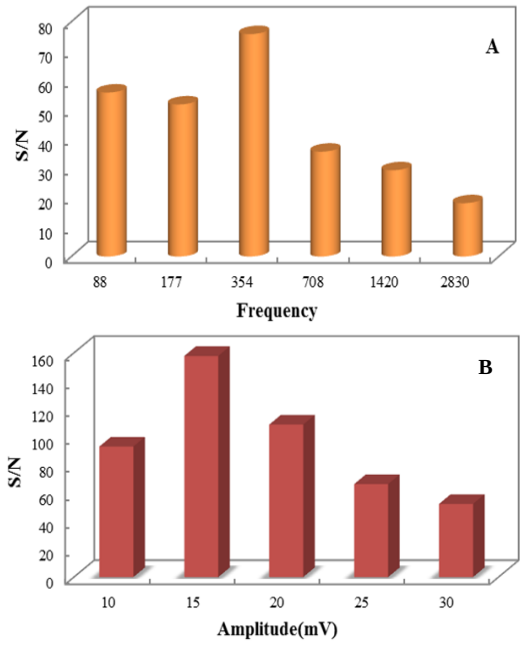

Figure 9. Results of frequency (A) and the amplitude (B) optimization tests for a 0.1 mM sulfadiazine solution in PBS (pH=10.0) using the $Tb_2(WO_4)_3$/CPE

3.8. Evaluating Reproducibility, repeatability and stability of the results

The reproducibility evaluations were performed through constructing 5 electrodes in 5 different days, and using them to analyze a 0.1 mM sulfadiazine solution and while recording the maximum current responses. The experiments revealed the relative standard deviation of the analyses to be 3.8%, reflecting the good reproducibility. For the repeatability test, one constructed $Tb_2(WO_4)_3$/CPE was prepared and examined 5 times in a single day, and the RSD of the peak currents was 1.02%. Under ambient conditions the electrode revealed to be stable for one month.

3.9. Calibration and detection limit

FFTSWV was used for sulfadiazine determination as highly sensitive method in which environmental noises were omitted by means of FFT technique and resulted to lower detection limit. The optimized FFTSWV parameters were employed to record the response current for the calibration curve of sulfadiazine in PBS (0.01 M, pH 10.0). As it is shown in Figure 10 (B) increasing the analyte concentration linearly boosted the oxidation current in two ranges from 0.01-1.0 μM and 1.0-100 μM. The equations of I(μA) = 6.0504[sulfadiazine (μM)] +5.0908 and I(μA) = 3.8969[sulfadiazine (μM)] +4.8513 was fitted in calibration plots which implied a sensitivity of 6.0504 and 3.8969 μA μM^{-1}, respectively.

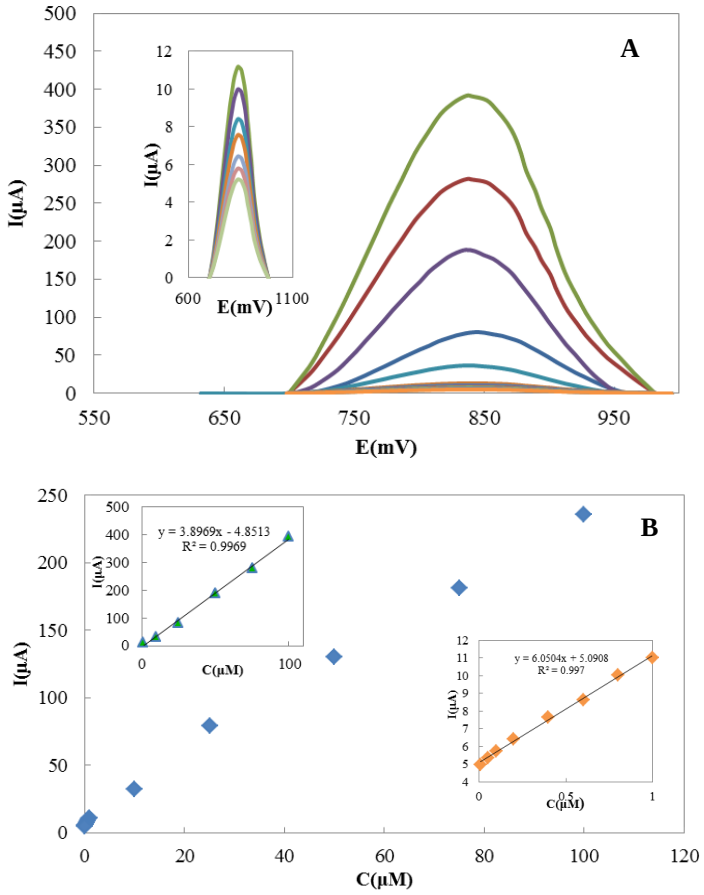

Figure 10. (A) Fast Fourier transform Square wave voltammograms (B) Calibration curve observed for 0.01-100.0 µM sulfadiazine (from inside to outside) in 0.01 M phosphate buffer (pH 10.0) at $Tb_2(WO_4)_3$/CPE

Table 1. The efficiency values reported in previous reports on the electrochemical determination of sulfadiazine

Electrode	**Method**	**E (mV)**	**LOD**	**Linear range**	**Ref.**
Boron-doped diamond (BDD)	Square-wave voltammetry	1100	2.19 µM	8.01µM-1.19 mM	[31]
MIP-modified carbon paste electrode	CV and DPV[a]	920	0.14 µM	0.2µM-1.0 mM	[34]
DMF/carboxyl/MWCNTs/GCE	CV and EIS[b]	963	0.067 µM	0.5µM-0.1 mM	[39]
PFR/CPE[c]	CV and EIS	990	1.47 µM	4.98-47.6 µM	[40]
$Tb_2(WO_4)_3$/CPE	CV and FFTSWV	850	0.004 µM	0.01-1.0 µM 1.0-100 µM	This work

a. Differential pulse voltammetry, b. Electrochemical impedance spectroscopy, c. Porphyrin carbon paste electrode

The detection limit was defined as S_b/m where S_b is the standard deviation recorded for the blank signal, and *m* expresses the slope of the calibration curve. This parameter was determined as 4.10 nM. The obtained LOD for sulfadiazine is considerably less than those reported in other reports as summarized in Table 1.

3.10. Potential interferences study

The accuracy of the sensor is under the impact of analytical selectivity. For this purpose, the effect of various possible interferences on the sulfadiazine determination were studied. The concentration of interfering species caused less than 5% relative error in electrode response, evaluated as tolerance limit. The acceptable tolerance limit was obtained for 1000-fold concentrations of Mg^{2+}, Na^{+}, K^{+}, Ca^{2+}, CO_3^{2-}, H_2PO^{4-}, NO_3^{-}, I^{-}, Cl^{-}; 100-fold excess concentrations of glucose and maltose; 40 and 20-fold concentrations uric and ascorbic acids, respectively. The results (Table 2) revealed that the performance of the modified electrode was not considerably affected in the presence of the mentioned species.

Table 2. Interference results for a 0.01 mM solution of sulfadiazine in PBS (pH =10.0) using the $b_2(WO_4)_3$/CPE, in the presence of the mentioned concentrations of each species

Species	**Tolerance limits ($C_{species}/C_{naproxen}$)**
Mg^{2+}, Na^{+}, K^{+}, Ca^{2+} CO_3^{2-}, $H_2PO_4^{-}$, NO_3^{-}, I^{-}, Cl^{-}	1000
Glucose, Maltose	100
Uric acid	50
Ascorbic acid	30

3.11. Performance of proposed electrode in real sample analysis

The performance of the sensor was checked in sulfadiazine tablet solution (Table 3). The test solution was prepared as mentioned above, and known amounts of sulfadiazine were added to the 1.5 µM sulfadiazine solutions according to the standard addition method and the recovery values were determined.

Table 3. Determination of sulfadiazine in real sample by standard addition method

Sulfadiazine added (µM)	**Sulfadiazine found (µM)**	**Recovery (%)**	**RSD%[a]**
-	1.4	_	1.8
19.4	20.4	97.9	1.6
37.9	38.8	98.7	1.3
56.6	58.3	100.5	0.9
73.7	76.4	101.8	0.7

[a]RSD determined for n=4

4. CONCLUSION

In the present study, $Tb_2(WO_4)_3$ modified CPE was developed as a highly sensitive sensor for the voltammetric determination of sulfadiazine. Analysis by FFTSWV technique and the present sensor resulted in low detection limit of 4.10 nM which indicated that the modified electrode is very sensitive and suitable for the analysis of trace amounts of sulfadiazine. In comparison with the other recent works, in addition to good reproducibility, fast response time and simplicity, the detection limit was considerably lower than the previous reports. Therefore, the excellent electrochemical efficiency of the $Tb_2(WO_4)_3$ nanoparticles make it a promising candidate for sulfadiazine electrochemical sensing.

Acknowledgments

The authors gratefully thank the University of Tehran Research Council for their support in this work.

Declarations of interest

The authors declare no conflict of interest in this reported work.

REFERENCES

[1] A. Marzo, and L. Dal Bo, J. Chromatogr. A 812 (1998) 17.
[2] T.G. Diaz, A.G. Cabanillas, M.I.A. Valenzuela, and F. Salinas, Analyst 121 (1996) 547.
[3] J.D. Voorhies, and R.N. Adams, Anal. Chem. 30 (1958) 346.
[4] W. De-Keizer, M.E. Bienenmann-Ploum, A.A. Bergwerff, and W. Haasnoot, Anal. Chim. Acta 14 (2008) 142.
[5] U. Koesukwiwat, S. Jayanta, and N. Leepipatpiboon, J. Chromatogr. A 1140 (2007) 147.
[6] H. Amini, and A. Ahmadiani, J. Pharm. Biom. Anal. 43 (2007) 1146.
[7] A. Preechaworapun, S. Chuanuwatanakul, Y. Einaga, K. Grudpan, S. Motomizu, and O. Chailapakul, Talanta 68 (2006) 1726.
[8] V.B. Reeves, J. Chromatogr. B 723 (1999) 127.
[9] B. Chiavarino, M.E. Crestoni, A. Marzio, and S. Fornarini, J. Chromatogr. B 706 (1998) 269.
[10] N. Assassi, A. Tazerouti, and J.P. Canselier, J. Chromatogr. A 1071 (2005) 71.
[11] T.Y. You, X.R. Yang, and E.K. Wang, Analyst 123 (1998) 2357.
[12] A. Wong, C. A. Razzino, T. A. Silva, and O. Fatibello-Filho, Sens. Actuators B Chem. 231 (2016) 183.
[13] S. Jafari, F. Faridbod, P. Norouzi, A. Shiralizadeh Dezfuli, D. Ajloo, F. Mohammadipanah, and M.R. Ganjali, Anal. Chim. Acta 895 (2015) 80.

[14] V.K. Gupta, P. Norouzi, H. Ganjali, F. Faridbod, and M.R. Ganjali, Electrochim. Acta 100 (2013) 29.
[15] P. Norouzi, G.R. Nabi Bidhendi, M.R. Ganjali, A. Sepehri, and M. Ghorbani, Microchim. Acta 152 (2005) 123.
[16] P. Norouzi, M.R. Ganjali, and L. Hajiaghababaei, Anal. Lett. 39 (2006) 1941.
[17] P. Norouzi, M.R. Ganjali, T. Alizadeh, and P. Daneshgar, Electroanalysis 18 (2006) 947.
[18] P. Norouzi, F. Faridbod, B. Larijani, and M.R. Ganjali, Int. J. Electrochem. Sci. 5 (2010) 1213.
[19] P. Norouzi, M.R. Ganjali, and P. Matloobi, Electrochem Commun, 7 (2005) 333.
[20] C. Esmaeili, P. Norouzi, M.S. Zar, M. Eskandari, F. Faridbod, and M.R. Ganjali, J. Electrochem. Soc. 166 (2019) B1630
[21] P. Norouzi, H. Ganjali, B. Larijani, M.R. Ganjali, F. Faridbod, and H.A. Zamani, Int. J. Electrochem. Sci. 6 (2011) 5189
[22] P. Norouzi, V.K. Gupta, B. Larijani, S. Rasoolipour, F. Faridbod, and M.R. Ganjali, Talanta 131 (2015) 577.
[23] P. Norouzi, M. Pirali-Hamedani, M.R. Ganjali, and F. Faridbod, Int. J. Electrochem. Sci. 5 (2010) 1434.
[24] P. Norouzi, B. Larijani, M.R. Ganjali, and F. Faridbod, Int. J. Electrochem. Sci. 7 (2012) 10414.
[25] P. Norouzi, V.K. Gupta, F. Faridbod, M. Pirali-Hamedani, B. Larijani, and M.R. Ganjali, Anal. Chem. 83 (2011) 1564.
[26] G. Chen, X. Hao, B. L. Li, H. Q. Luo, and N.B. Li, Sens. Actuators B: Chem. 237 (2016) 570.
[27] K. Skrzypczyńska, K. Kuśmierek, and A. Świątkowski, J. Electroanal. Chem. 766 (2016) 8.
[28] J. H. Luo, X. X. Jiao, N. B. Li, and H.Q. Luo, J. Electroanal. Chem. 689 (2013) 130.
[29] M.R. Ganjali, H. Beitollahi, R. Zaimbashi, S. Tajik, M. Rezapour, and B. Larijani, Int. J. Electrochem. Sci. 13 (2018) 2519.
[30] V. Arabali, M. Ebrahimi, M. Abbasghorbani, V.K. Gupta, M. Farsi, M.R. Ganjali, and F. Karimi, J. Mol. Liq. 213 (2016) 312.
[31] H.C. Aspinall, Chemistry of the f-block elements, CRC Press (2001).
[32] M. R. Ganjali, V. K. Gupta, F. Faridbod, and P. Norouzi, Lanthanides series determination by various analytical methods, Elsevier Inc., Cambridge, MA 02139, USA (2016).
[33] V. K. Gupta, P. Norouzi, H. Ganjali, F. Faridbod, and M.R. Ganjali, Electrochemical Acta, 100 (2013) 29.
[34] M. Rahimi-Nasrabadi, V. Pourmohamadian, M. Sadeghpour Karimi, H. R. Naderi, M. A. Karimi, K. Didehban, and M.R. Ganjali, J. Mater. Sci. Mater. Electron. 28 (2017) 12391.

[35] V.F. Lvovich, Impedance Spectroscopy: Application to Electrochemical and Dielectric Phenomena, John Wiley & Sons, Inc, Hoboken, New Jersey (2012).
[36] A.J. Bard, and L.R. Faulkner, Electrochemical Methods, Fundamentals and Applications, Second ed. ed., Wiley, New York (2001).
[37] E. Laviron, J. Electroanal. Chem. 101 (1979) 19.
[38] C.D. Souza, O.C. Braga, I.C. Vieira, and A. Spinelli, Sens. Actuators B 135 (2008) 66.
[39] B. He, and S. Yan, Int. J. Electrochem. Sci. 12 (2017) 3001.
[40] D. Lima, L.C. Lopes, C.G. De Jesus, C.M.F. Calixto, G.N. Calaça, A.G. Viana, C.A. Pessôa, Revista Virtual de Quimica 8 (2016) 1660.